

High-Energy Threshold Reaction Rates on 0.8 GeV Proton-Irradiated Thick W and W-Na Targets

YU.E. TITARENKO*, V.F. BATYAEV, E.I. KARPIKHIN, V.M. ZHIVUN, A.B. KOLDOBSKY, R.D. MULAMBETOV, S.V. MULAMBETOVA, S.L. ZAITSEV, S.G. MASHNIK¹, R.E. PRAEL¹

Institute for Theoretical and Experimental Physics (ITEP), B.Chermushkinskaya 25, 117259 Moscow, Russia
¹*Los Alamos National Laboratory, Los Alamos, NM 87545, USA*

Abstract Results are presented of measuring the threshold activation reaction rates in ¹²C, ¹⁹F, ²⁷Al, ⁵⁹Co, ⁶³Cu, ⁶⁵Cu, ⁶⁴Zn, ⁹³Nb, ¹¹⁵In, ¹⁶⁹Tm, ¹⁸¹Ta, ¹⁹⁷Au, and ²⁰⁹Bi experimental samples placed along the axis inside and outside the 0.8 GeV proton-irradiated 92-cm thick W-Na and 4-cm thick W targets. 158 reactions of up to ~0.5 GeV thresholds have been measured in 123 activation samples for W-Na target, and 157 reactions in 36 activation samples for W target. The reaction rates were determined using the γ -spectrometry method. In total, more than 1000 values of activation reactions were determined in the experiments. In both cases the measured reaction rates were compared with the LAHET code simulated rates and using several nuclear databases for the respective excitation functions, namely, ENDF/B6 for cross section of neutrons at energies below 20 MeV and MENDL2 together with MENDL2P for cross sections of protons and neutrons of 20 to 100 MeV energies. A general satisfactory agreement between simulated and experimental data has been found. Nevertheless, further studies should be aimed at perfecting the simulation of the production of the secondary protons and high-energy neutrons, especially in the sideward and backward directions with respect to the beam. The results obtained permit some conclusions concerning the reliability of the transport codes and databases used to simulate the ADS with Na-cooled W targets. The high-energy threshold excitation functions to be used in the activation-based unfolding of neutron spectra inside the ADS can also be inferred from the results.

I. INTRODUCTION

The pending researches with the pilot Accelerator Driven Systems (ADS) require reliable nuclear data. One of the possible fields of the data application is the activation-based unfolding of the high-energy (up to ~1 GeV) neutron spectra inside the ADS target and the near-target blanket zone. The high-energy “tail” in the ADS spectra triggers the high-energy threshold (>10 MeV) reactions, which are not studied in detail in the conventional reactor researches. Therefore, the excitation functions that may be derived from high-energy calculations, or retrieved from the available databases require insistently a reliable verification via testing experiments with the high-energy proton-irradiated target micromodels.

The ITEP U-10 proton synchrotron was used to realize a run of experiments to study the threshold activation reaction rates inside and outside thick W and W-Na targets.

II. EXPERIMENT

The W-Na target was assembled of alternating cylindrical W and Na discs (see Fig. 1A). The displayed succession of the disks was selected to obtain the maximum attainable uniform neutron distribution along the target. The W discs are the 150-mm diameter full-metal structures of 40-mm (7 pieces) and 20-mm (5 pieces) thicknesses. The Na discs (13 pieces) are the 150-mm diameter, 40-mm thick thin-walled cylindrical containers made of 0.5-mm thick stainless sheet steel, filled with metallic Na, and soldered tight. The experimental activation samples are 10.5-mm or 10.0-mm diameter circular discs cut of metal foils of the certified composition. During the irradiation runs, the samples were placed on the W disc surfaces and in their seats milled in the rulers (see Fig. 2). In the experiments, the activation reaction rates were determined on the ²⁰⁹Bi, ¹⁹⁷Au, ¹⁶⁹Tm, ¹¹⁵In, ⁹³Nb, ⁶⁵Cu, ⁶⁴Zn, ⁶³Cu, ⁵⁹Co, ²⁷Al, ¹⁹F, and ¹²C nuclides. Besides, the ²²Na production rate in the Na discs was determined.

The W target is a single W disk of 150-mm diameter and 40-mm thickness. The same experimental activation samples, except ¹⁶⁹Tm and ¹⁸¹Ta, were placed on the W-disk, as shown in Fig. 1B.

* Corresponding author: E-Mail Yury.Titarenko@itep.ru

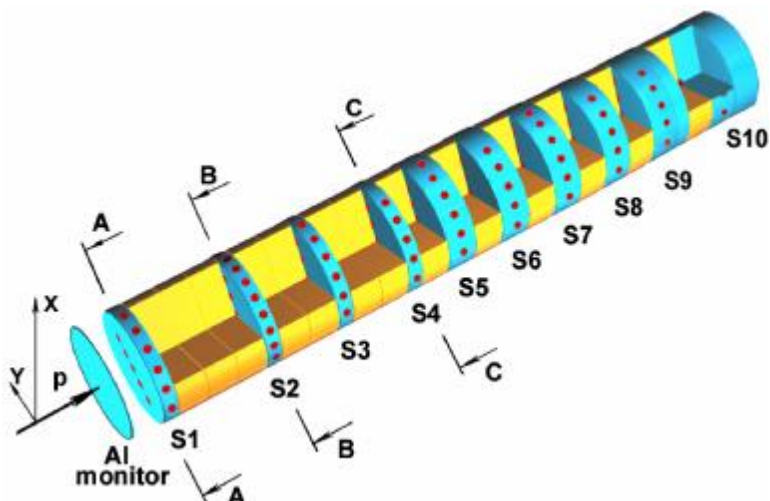


Fig 1A. The W-Na target assembly view.

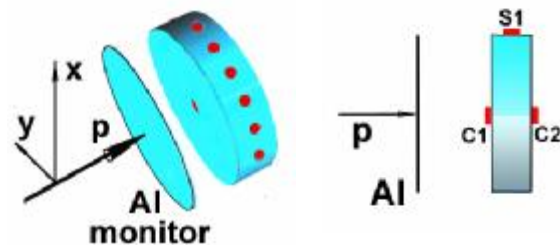


Fig 1B. A schematic of the arrangement and irradiation of the samples of a single W disc.

Both targets were irradiated with the ITEP synchrotron-extracted 0.8 GeV proton beam. The W-Na and W irradiations lasted for 10 h and 2 h, respectively. The proton number on the targets was found to be $(6.5 \pm 0.4) \times 10^{14}$ for W-Na target and $(6.0 \pm 0.4) \times 10^{13}$ for W target. The irradiated activation samples were γ -spectrometered using the Ge and Ge-Li detector-based high-resolution spectrometers. The details of target composition, experimental layout, irradiation parameters, measuring technique and reaction rates determining can be found in ^{1, 2)}.

In total, 979 and 296 values of the reaction rates have been determined in the W-Na and W experiments, respectively (see Table 1). Comparison was made between the sets of the high-threshold reaction rates in the case of identical arrangement of the respective samples in the W and W-Na targets. Fig. 3 shows the reaction rates in Bi and In measured at point S1 in both experiments. It should be noted that the excess of the reaction rates in W over W-Na rises as the reaction threshold increases. In the case of the high-threshold reactions (with $E_{th} > 200$ MeV), the experimental W – to – W-Na reaction rate ratio reaches a few unities.

Table 1. List of the reaction rates measured.

Nuclide	The products for the reaction rates measured	Number of values	
		W-Na	W
²⁰⁹ Bi	²⁰⁷ Po, ²⁰⁶ Po, ²⁰⁶ Bi(i,c), ²⁰⁵ Bi, ²⁰⁴ Bi, ²⁰³ Bi, ²⁰³ Pb(i,c), ²⁰¹ Pb, ²⁰⁰ Pb, ²⁰² Tl, ²⁰⁰ Tl(i,c), ¹⁹¹ Pt, ⁹⁶ Tc, ⁹⁶ Nb, ⁸² Br	165	14
¹⁹⁷ Au	¹⁹⁸ Au, ¹⁹⁶ Au, ¹⁹⁴ Au, ¹⁹¹ Pt	33	6
¹⁸¹ Ta	¹⁸² Ta, ^{178m} Ta, ¹⁷⁶ Ta, ¹⁷⁵ Ta, ¹⁷³ Ta, ^{180m} Hf, ¹⁷⁵ Hf, ¹⁷³ Hf, ¹⁷⁰ Hf, ¹⁷² Lu, ¹⁷¹ Lu, ¹⁶⁹ Lu, ¹⁶⁷ Tm, ¹⁶⁵ Tm, ¹⁶¹ Er	112	-
¹⁶⁹ Tm	¹⁶⁶ Yb, ¹⁶⁸ Tm, ¹⁶⁷ Tm, ¹⁶⁶ Tm(i,c), ¹⁶⁵ Tm, ¹⁶³ Tm, ¹⁶¹ Er, ¹⁶⁰ Er, ^{160m} Ho(i,c), ¹⁵⁷ Dy, ¹⁵⁵ Dy, ¹⁵³ Dy, ¹⁵² Dy, ¹⁵³ Tb, ¹⁵² Tb, ¹⁵¹ Tb, ¹⁵⁰ Tb	19	-
¹¹⁵ In	¹¹³ Sn, ¹¹⁶ In, ^{115m} In(i,c), ^{114m} In, ^{113m} In(i,c), ¹¹¹ In, ¹¹⁰ In, ¹⁰⁹ In, ¹¹⁵ Cd, ¹¹¹ Ag, ^{110m} Ag, ^{106m} Ag, ¹⁰⁵ Ag, ¹⁰¹ Pd, ¹⁰⁰ Pd, ¹⁰¹ Rh, ¹⁰⁰ Rh(i,c), ⁹⁹ Rh, ⁹⁷ Ru, ⁹⁶ Tc, ⁹⁵ Tc, ⁹⁰ Mo, ⁹⁹ Nb(i,c), ⁸⁹ Zr, ⁸⁷ Y	207	119
⁹³ Nb	⁹⁰ Nb, ⁸⁹ Zr, ⁸⁶ Zr, ⁹⁰ Y, ^{87m} Y, ⁸⁷ Y, ⁸⁶ Y(i,c)	8	21
⁶⁵ Cu	⁶⁴ Cu, ⁶¹ Cu, ⁶⁵ Ni, ⁵⁸ Co, ⁵⁷ Co, ⁵⁶ Co, ⁵⁵ Co, ⁵⁶ Mn, ⁵² Mn, ^{44m} Sc, ⁴⁴ Sc(i,m+g)	12	9
⁶⁴ Zn	⁶⁵ Zn, ⁶³ Zn, ⁶² Zn, ⁶⁴ Cu, ⁶¹ Cu, ⁶⁰ Cu, ⁵⁷ Ni, ⁵⁸ Co, ⁵⁷ Co, ⁵⁶ Co, ⁵⁵ Co, ⁵⁶ Mn, ⁵² Mn, ⁴⁸ Cr, ^{44m} Sc, ⁴⁴ Sc(i,m+g)	17	18
⁶³ Cu	⁶¹ Cu, ⁵⁸ Co, ⁵⁵ Co, ⁵² Mn	4	13
⁵⁹ Co	⁵⁷ Ni, ⁵⁸ Co(i,m+g), ^{58m} Co, ⁵⁷ Co, ⁵⁶ Co, ⁵⁵ Co, ⁵⁹ Fe, ⁵² Fe, ⁵⁶ Mn, ⁵² Mn, ⁵¹ Cr, ⁴⁸ Cr, ⁴⁸ V, ⁴⁸ Sc, ⁴⁷ Sc(i,c), ⁴⁶ Sc, ^{44m} Sc, ⁴⁴ Sc(i,m+g), ⁴³ Sc, ⁴⁷ Ca, ⁴³ K, ²⁴ Na, ⁷ Be	222	73
²⁷ Al	²⁷ Mg, ²⁴ Na, ²² Na, ⁷ Be	186	21
¹⁹ F	¹⁸ F	1	1
¹² C	¹¹ C	1	1
Total		979	296

Then, the simulated reaction rates may then be determined via the integral multiplication of the calculated spectra by the respective reaction σ cross sections: $R_x = R_{n,x} + R_{p,x} = \sum_{i=n,p} \int \sigma_{i,x}(E) \cdot \varphi_i(E) dE$. The required proton

and neutron excitation functions $\sigma_{i,x}(E)$ were accumulated using:

- the MENDL2⁴) and MENDL2p⁵) databases, which give the neutron and proton reaction excitation functions up to 100 MeV and 200 MeV, respectively;
- the LAHET code simulated excitation functions from 100 MeV to 800 MeV;
- the available experimental data on the production cross sections of the respective reaction products (the EXFOR database).

Basing on the above dataset for a particular reaction, we can select the excitation function that would be consistent with all the data and agree satisfactorily with the experimental reaction rates at all measurement points.

The following two groups of reactions, whose cross sections are determined by different algorithms, can tentatively be singled out.

1. The reactions supported by sufficient experimental proton cross section data throughout the necessary energy range. The MENDL and LAHET excitation functions are, then, normalized and joined to each other, so that they would optimally describe the set of experimental points. In this case, the same normalization parameters were also applied to the neutron excitation functions that are not supported by any experimental points.

2. The reactions supported by meager, or even none of, experimental data. In this case, where the comparison between experimental and calculated reaction rates shows systematic deviations of calculations from experiment, LAHET and MENDL were used to normalize the excitation functions in such a manner that the deviations would be minimized.

Our earlier work¹⁾ describes the reaction rates simulation algorithm in details.

IV. COMPARISON BETWEEN EXPERIMENT AND CALCULATIONS

Our earlier work¹⁾ has shown that most of the experimental results can be simulated to within a satisfactory accuracy (almost a half of the calculated data differ from experiment by less than 30%). The present work deals only with the reactions, for which a significant disagreement with experiments is observed (Fig. 5).

1. The calculated $^{209}\text{Bi}(p,3n)^{207}\text{Po}$ and $^{209}\text{Bi}(p,4n)^{206}\text{Po}$ reaction rates in the first and eighth W discs are much underestimated compared with experiment. Since ^{207}Po and ^{206}Po cannot be produced in neutron reactions on ^{209}Bi , we think that the discrepancy has arisen most probably from the fact that the LAHET code simulates rather inadequately the secondary proton production in backward direction in a hadron-nucleus cascade. Fig. 3 demonstrates the extremely low simulated proton flux on the surface of the first W disc (point S1).

2. From Figs. 5 it follows that point S1 is characterized by a significant underestimation of the data calculated for not only the proton-induced reactions proper, but also the high-threshold (~ 100 MeV and higher) mixed-type reactions. Table 3 is the list of the reactions. The disagreement can be explained by Fig. 3 (the third panel), which shows the neutron and proton spectra at points S1 and S2. The comparison between the neutron spectra at the two points indicates that, up to ~ 50 MeV, the S2 neutron flux density is about twice the S1 neutron flux density, in a good agreement with the R_{S1}/R_{S2} ratio for the moderate-threshold reactions ($^{27}\text{Al} \rightarrow ^{24}\text{Na}$ from Al, for instance). As neutron energy increases, however, the difference between the S1 and S2 flux densities rises, with the S1 flux vanishing at ~ 300 MeV. If the S1 neutron flux was actually as shown in Fig 3, the reactions with thresholds above ~ 200 - 300 MeV would have never been observed at point S1 (for example, $^{115}\text{In} \rightarrow ^{87}\text{Y}$, a ~ 400 MeV threshold). The significant experimental rates of the high-threshold reactions indicate that the simulated S1 neutron spectrum above ~ 100 MeV is much underestimated

Table 3. Comparison between experimental and calculated rates of high-threshold reactions at point S1.

Reactions	Threshold, MeV	Underestimation factor
^{201}Pb , ^{200}Pb , $^{200}\text{Tl}(i,c)$ from ^{209}Bi ; ^{173}Ta , ^{173}Hf , ^{167}Tm from ^{181}Ta	50 – 100	2 – 5
^{191}Pt from ^{209}Bi ; ^{101}Pd , $^{100}\text{Rh}(i,c)$ from ^{115}In	100 – 200	10 – 50
^{100}Pd , ^{97}Ru , ^{96}Tc , ^{95}Tc , ^{90}Nb , ^{87}Y from ^{115}In	200 and higher	100 and higher

The above mentioned difference in the reaction rates at point S1 in the W and W-Na experiments made us compare the high-energy part of the neutron spectra at that point. The considerable excess of the above presented reaction rates at point S1 indicates a significant difference in the high-energy parts of the neutron spectra. A detailed comparison between the spectra is shown in Fig. 6 as the ratio of the spectra at point S1 and the ratio of experimental reaction rates. A steady rise of the ratio of the simulated spectra with increasing neutron energy (from 1.6 at $E_n = 10$ MeV to ~ 2.5 at $E_n = 300-400$ MeV) is quite evident. At the same time, the ratio of the experimental reaction rates in the 300-700 MeV range reaches ~ 8 . So, the calculated spectral hardening proved to be, as a minimum, 3 times as low as that observed experimentally. To clarify the causes of the resultant discrepancies, Fig. 7 presents the calculated neutron spectra at points S1 and S2 for the W-Na target together with the experimental and calculated double-differential neutron production cross sections in W at 0,8 GeV. In the case of the double-differential cross sections, the agreement between calculations and experiment is much better, permitting us to conclude that the LAHET simulation of neutron production in all directions cannot give rise to the above mentioned discrepancies.

In our opinion, the LAHET description of the high-energy neutron transport in the W discs is predominantly responsible for the discrepancies. Particularly, this may concern the processes of high-energy neutron scattering from the range of small angles. The noted assumption will be studied in details in further works.

V. CONCLUSION

The results presented above indicate that, with rare exclusions, the described approaches make it possible to obtain the excitation functions of high-energy threshold reactions that lead to a satisfactory description of the measured reaction rates. The functions can be used to unfold the neutron spectra at different points inside the ADS.

Further studies should nevertheless be aimed at perfecting the simulation of the production of secondary protons and high-energy neutrons, especially in the sideward and backward direction with respect to the beam. This is emphasized by the data on the rates of Po production from Bi and of high-threshold reactions sidewise of the beam entry to the target.

It should be noted that the satisfactory agreement in the reaction rates is somewhat conditional in the case of lacking reliable experimental data on excitation function for Bi, In, Ta, etc. Therefore, additional high-energy experiments are required to measure the production cross section of secondary product nuclei and the reaction rates in the integral experiments with other target types.

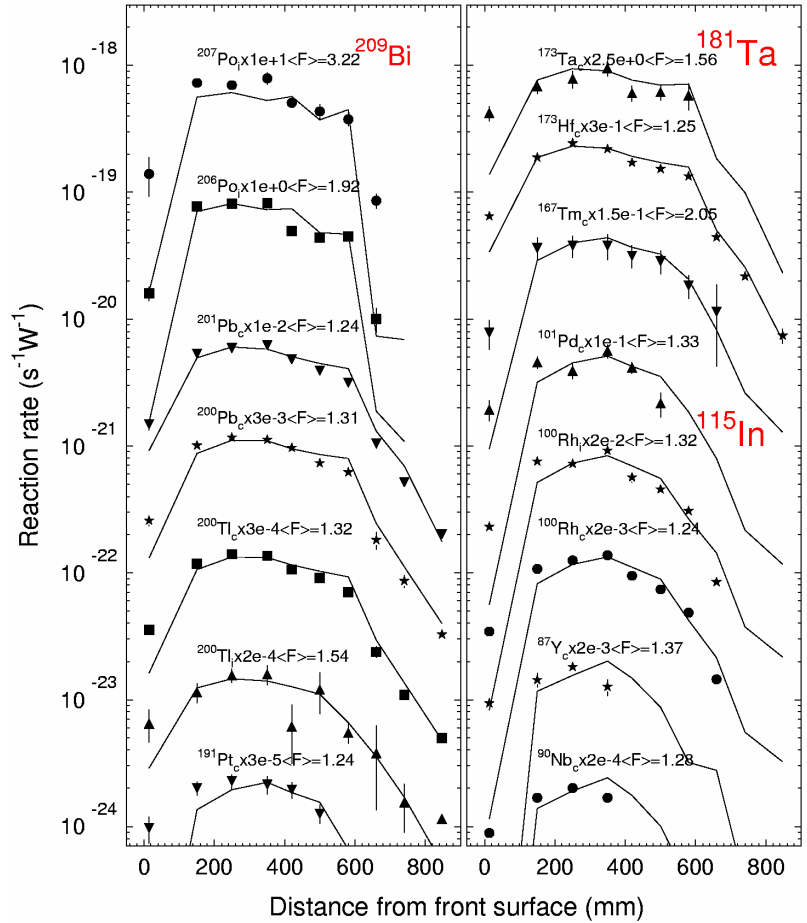


Fig. 5. The calculated and experimental reaction rates. The mean squared deviation factor $\langle F \rangle$ are presented for each reaction

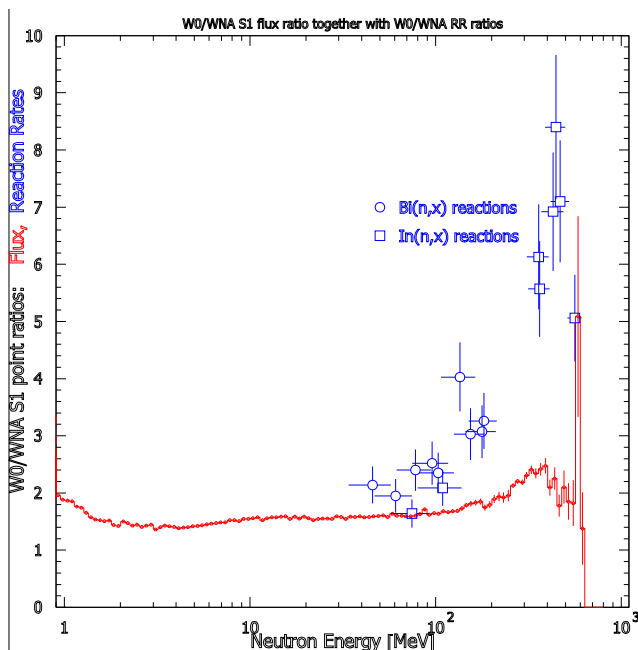


Fig. 6. The LAHET-simulated ratios of the neutron spectrum at point S1 for W target to the spectrum for W-Na target (the red line). The ratios of experimental reaction rates in Bi and In samples at point S1 for W target to the ratios of the same reactions for W-Na target. Plotted as abscissa is the characteristic energy at which a reaction proceeds.

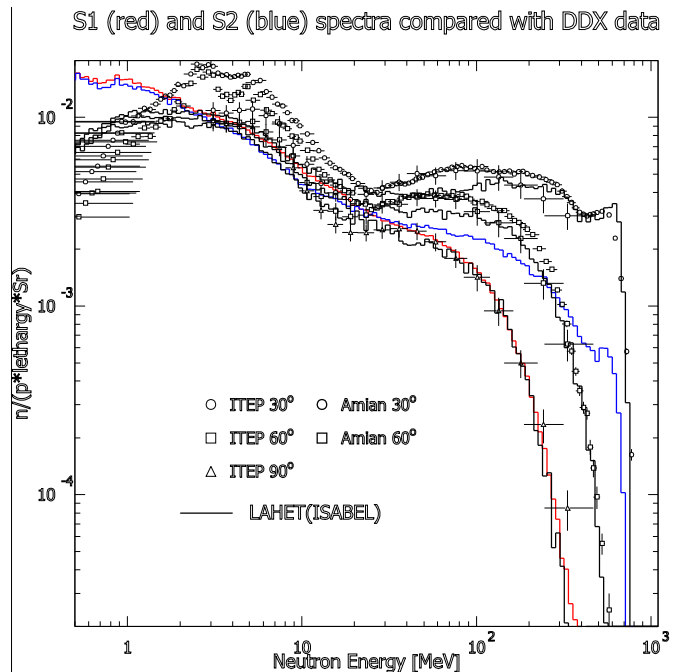


Fig. 7. The simulated neutron spectra at points S1 (the red line) and S2 (the blue line) for W-Na target and the experimental and calculated double-differential cross sections for neutron production in W at angles 30°, 60°, and 90° at proton energy 0.8 GeV. The experimental data are from the works of ITEP⁶⁾ and LANL⁷⁾.

ACKNOWLEDGEMENT

The authors are indebted to Dr. F.E.Chukreev (Kurchatov Institute) for his assistance in working with the EXFOR database.

The work has been supported by International Science and Technology Center (ISTC) under Project#1145. In addition, the work was partly supported by the U.S. Department of Energy.

REFERENCES

1. Yu.E. TITARENKO, et al., Threshold Activation Reaction and Absorption Dose Rates Inside and on the Surface of a Thick W-Na Target Irradiated with 0.8 GeV Protons, AccApp'03 Annual Meeting, San Diego, 1-5 June 2003, CA, USA; LANL Report **LA-UR-03-3402**; *nucl-ex/0305025*.
2. Yu.E. TITARENKO et al., Cross sections for nuclide production in 1GeV proton irradiated ²⁰⁸Pb, Phys. Rev. **C65** (2002) 064610; Yu.E. TITARENKO et al., Experimental and Computer Simulation Study of the Radionuclides Produced in Thin ²⁰⁹Bi Targets by 130 MeV and 1.5 GeV Proton-Induced Reactions. Nucl. Instr. Meth. **A414**, 73-99 (1998).
3. R.E. PRAEL, H. LICHTENSTEIN, User guide to LCS: The LAHET Code System, LANL Report **LA-UR-89-3014** (1989).
4. Yu.N. SHUBIN et al., Cross Section Data Library MENDL-2 to Study Activation and Transmutation of Materials Irradiated by Nucleons of Intermediate Energies, IAEA, INDC(CCP)-385, Vienna, May 1995.
5. Yu.N. SHUBIN et al., Cross Section Data Library MENDL-2p to Study Activation and Transmutation of Materials Irradiated by Nucleons of Intermediate Energies, Nuclear Data for Science and Technology (Trieste 1997), IPS, Bologna, 1997, v.1., p.1054.
6. Yu.V. TREBUKHOVSKY et al., PrePrint ITEP 2003-03.
7. W.B. AMIAN et al., Nucl.Sci.Eng. 112, 78 (1992); Nucl.Sci.Eng. 115, 1 (1993).